Electron Tunneling into Superconducting Mercury Films*†

STUART BERMON‡ AND D. M. GINSBERG
Department of Physics, University of Illinois, Urbana, Illinois
(Received 12 March 1964)

Tunneling measurements have been made on junctions consisting of evaporated films of aluminum and mercury separated by an aluminum oxide insulating layer. The width of the superconducting mercury energy gap extrapolated to $T=0°K$ has been determined to be $2\Delta(0)=(1.65\pm0.04)\times10^{-3}$ eV$=(4.60\pm0.11)k_BT_c$ from the current-voltage characteristic with the junction in the superconductor-insulator-superconductor configuration. Comparison is made with theory, and with thermodynamic and spectroscopic measurements of the gap. Measurements of the differential conductance in the vicinity of the gap in the metal-insulator-superconductor configuration show qualitative agreement with curves calculated from a BCS density of states, although the experimental curves are more peaked and have a larger tail at low bias voltages. The temperature dependence of the gap, as indicated by the differential conductance at zero bias, has been found to agree closely with the BCS variation, provided that the BCS curve is scaled by a constant multiplier. Structure, thought to be related to the phonon spectrum of mercury, has been observed in the first and second derivatives of the tunneling current.

I. INTRODUCTION

THE use of the electron tunneling technique to investigate the properties of superconductors is now well known.[1] In a tunneling experiment, the surface of one metal is oxidized to form an insulating layer, over which a second metal is deposited to form a metal-insulator-metal sandwich. If a voltage is then applied between the two metals, the quantum-mechanical tunneling effect will cause a current to flow. If both metals are in the normal state, the current versus voltage characteristic (I versus V) will be approximately linear for small voltages. If one of the metals is made superconducting, the characteristic becomes nonlinear, and its slope dI/dV is directly related to the superconducting density of states. With both metals in the superconducting state, the characteristic exhibits a negative-resistance region which can be used to determine directly the width of the superconducting energy gaps in the two superconductors.

The precise voltage dependence of dI/dV in various superconductors will ultimately provide a valuable test for the validity of theories concerning the nature of the electron-phonon interaction,[2–4] including retardation[5] and lifetime effects, and of theories describing the tunneling process itself.[6–9] Small structure on the tunneling curves at energies above the gap provides useful information concerning the superconductor's phonon spectrum, and its influence on the effective tunneling density of states.[10] (Our tunneling junctions are not of low enough resistance to yield information about the Josephson effect,[11] phonon-assisted tunneling,[12] or multiparticle tunneling.[13,14])

The properties of superconducting mercury as determined by the electron-tunneling technique are the subject of this paper. Mercury and lead both possess relatively high ratios of critical temperature to Debye temperature, and are of special interest because of their anomalous thermodynamic behavior in the superconducting state, which is thought to be related to the strong electron-phonon interaction in these metals. Curves showing their critical magnetic fields versus reduced temperature exhibit a positive deviation from a parabolic behavior, whereas other soft superconductors show a negative deviation[15] in good agreement with the prediction of the BCS theory.[16]

Lead has been extensively investigated through use of the tunneling technique. Mercury has not, probably because of the experimental difficulties involved in preparing tunneling sandwiches in which one of the metals is a liquid at room temperature. We have prepared junctions consisting of evaporated films of aluminum and mercury separated by an aluminum oxide insulating layer. Tunneling measurements have been made on these junctions in an effort to determine the width of the

* Supported in part by the National Science Foundation and the Alfred P. Sloan Foundation.
† Based on the Ph.D. thesis of S. Bermon, University of Illinois, 1964 (unpublished).
‡ Predoctoral National Science Foundation Fellow, present address, Massachusetts Institute of Technology Lincoln Laboratory.
[1] D. H. Douglass, Jr. and L. M. Falicov, in *Progress in Low Temperature Physics*, edited by C. J. Gorter (North-Holland Publishing Company, Amsterdam), Vol. IV (to be published).
[2] J. Bardeen and D. Pines, Phys. Rev. **99**, 1140 (1955).
[3] N. N. Bogoliubov, Zh. Eksperim. i Teor. Fiz. **34**, 58 (1958) [English transl.: Soviet Phys.—JETP **7**, 41 (1958)].
[4] G. M. Eliashberg, Zh. Eksperim. i Teor. Fiz. **38**, 966 (1960) [English transl.: Soviet Phys.—JETP **11**, 696 (1960)].
[5] P. Morel and P. W. Anderson, Phys. Rev. **125**, 1263 (1962).
[6] J. Bardeen, Phys. Rev. Letters **6**, 57 (1961).
[7] W. A. Harrison, Phys. Rev. **123**, 85 (1961).
[8] M. H. Cohen, L. M. Falicov, and J. C. Phillips, Phys. Rev. Letters **8**, 316 (1962).
[9] J. Bardeen, Phys. Rev. Letters **9**, 147 (1962).
[10] J. R. Schrieffer, D. J. Scalapino, and J. W. Wilkins, Phys. Rev. Letters **10**, 336 (1963).
[11] B. D. Josephson, Phys. Letters **1**, 251 (1962).
[12] L. Kleinman, Phys. Rev. **132**, 2484 (1963).
[13] B. N. Taylor and E. Burstein, Phys. Rev. Letters **10**, 14 (1963).
[14] J. R. Schrieffer and J. Wilkins, Phys. Rev. Letters **10**, 17 (1963).
[15] See J. Bardeen and J. R. Schrieffer, in *Progress in Low Temperature Physics*, edited by C. J. Gorter (North-Holland Publishing Company, Amsterdam, 1961), Vol. III.
[16] J. Bardeen, L. N. Cooper, and J. R. Schrieffer, Phys. Rev. **108**, 1175 (1957).

superconducting energy gap in the zero-temperature limit and as a function of temperature, and to measure the density of states both in the vicinity of the gap edge and at higher energies, where we have observed structure in the density of states which seems to yield information concerning the phonon distribution in mercury.

II. SAMPLE PREPARATION

The Al-Al_2O_3-Hg tunneling sandwiches in this experiment were prepared in a chamber housed in the bottom of a helium Dewar. The chamber served both as the evaporator and as the cryostat.

The films are deposited onto a well cleaned piece of z cut, optically polished, crystal quartz with dimensions $\frac{11}{16}$ in.$\times\frac{1}{2}$ in.$\times$0.045 in. thick. Initially, four gold electrodes are evaporated onto two substrates in a separate evaporator. These are then mounted opposite one another in a bakelite slide holder. Electrical contact is made to the gold electrodes by means of pressure contacts, consisting of strips of 0.0025-in.-thick gold sheet fastened to the underside of phosphor-bronze spring terminals.

A schematic drawing of part of the evaporator-cryostat is shown in Fig. 1. The slide holder, the filament lead plug holder, and the light trap are affixed to the $\frac{1}{8}$-in.-diam hollow Inconel turning shaft, which extends to the top of the apparatus, and which is used to position the slides for the various stages of the evaporation. Masks, $\frac{1}{64}$ in. below the slides, define the area of the films. The tunneling junction has an area of approximately 1 mm^2. The evaporation filaments are situated 3 in. below the slides.

The filament current leads pass down through the exhaust tube, and consist of No. 18 stranded copper wire insulated with fiberglass sleeving. At the conclusion of the evaporation these leads are drawn up through trap doors in the light trap to the top of the apparatus, since the heat leak from them would be considerable. A second method was later employed, in which the leads are brought down outside the exhaust tube. They then enter the evaporator-cryostat from the bottom through Stupakoff electrical feed-through seals, and make the connection with the filament posts via a plug-jack arrangement.

The filament for evaporating the aluminum consists of a coil of seven or eight loops made from two twisted strands of 0.015-in.-diam tungsten wire. The aluminum, in the form of 0.032-in.-diam wire (Baker and Company, ACS grade, 99.9%) is cut into $\frac{1}{2}$-in. segments, which are bent into a hairpin shape and hung from alternate loops. The mercury filament consists of a 4-mm-o.d., 1-mm-wall Pyrex tube, $\frac{1}{2}$ in. long, partially sealed off at the bottom and wound on the outside with six turns of 0.015-in.-diam tungsten wire. The mercury used in the evaporations was Reagent Grade ACS obtained from the National Lead Company (Analysis: Ag and Au 0.0005% max; base metals 0.0001% max).

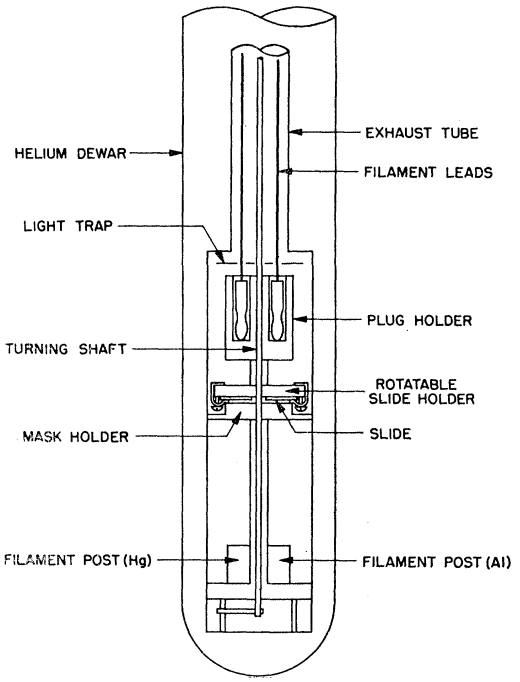

FIG. 1. Schematic drawing of the evaporator-cryostat.

After the aluminum and the mercury have been placed in their respective filaments, the system is sealed with a Wood's metal joint, placed in the Dewar, and connected to an oil diffusion pump and forepump through a liquid-nitrogen cold trap.

It is desirable to evaporate some of the metal charge prior to the actual film evaporation in order to expel absorbed gases and to rid the metal of surface contamination. For this purpose, a second slide (the dummy slide) is placed in the slide holder to serve as a monitor for the preliminary evaporations. (See Fig. 1.) The support for the mask holder prevents metal evaporating from one of the filaments from reaching more than one of the slides at a time.

Initially, some of the aluminum is evaporated onto the dummy slide. The slide holder is then rotated 180°, and the aluminum is evaporated onto the sample slide. The aluminum evaporation takes place at room temperature at pressures between 1×10^{-5} and 3×10^{-5} Torr. Evaporation rates are between 100 and 250 Å per sec, and final film thicknesses vary between about 1500 and 2500 Å.

After the aluminum has been evaporated, the cold trap is removed and the system is opened to the atmosphere for three minutes to permit oxidation of the aluminum film to form the Al_2O_3 barrier layer. The system is then pumped out and the inner Dewar is filled with liquid nitrogen. Helium exchange gas is let in to a pressure of a few Torr, causing the substrate and the remaining parts of the cryostat to cool to about 77°K within 15 min. In this way, the remaining condensable

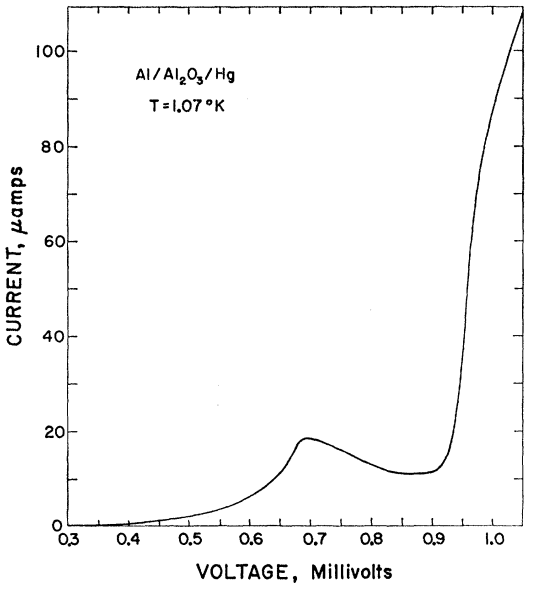

FIG. 2. Current versus voltage characteristic for the Al-Al_2O_3-Hg tunneling junction in the superconductor-insulator-superconductor configuration at $T=1.07°K$, for V in the range from 0.3 to 1.05 mV.

matter is deposited on the walls of the cryostat and not on the slides.

The system is then pumped down once more, some of the mercury is evaporated onto the dummy slide, the slide holder is rotated back 180°, and the sample film is evaporated. The pressure during the mercury evaporation is approximately 2×10^{-5} Torr. Very little heating of the substrate during the evaporation is observed (less than 2°K). Evaporation rates are from 100 to 300 Å per sec, and final mercury film thicknesses are between 1000 and 2000 Å. (The thickness of the mercury film was approximately determined by measuring the resistance at 77 and 4.2°K and using Matthiessen's rule.[17])

After the evaporation is completed, several Torr of helium exchange gas are let into the system to provide thermal contact. The outer Dewar is filled with liquid nitrogen, and the liquid nitrogen in the inner Dewar is forced out, so that it may be filled with liquid helium. At no time before it is discarded is the mercury film exposed to the air or heated above 77°K.

III. THE ENERGY GAP WIDTH AT LOW TEMPERATURE

The most unambiguous method of determining the width of the energy gap is the measurement of the I–V characteristic with both metals of the sandwich in the superconducting state.[18] In general, for two different superconductors, a and b, we expect to see a local maximum in the current when eV equals the difference of the energy gaps, $|\Delta_a-\Delta_b|$, followed by a negative resistance region and then a sharp increase in the current when $eV=\Delta_a+\Delta_b$.

Figure 2 shows an experimental plot of I versus V for an Al-Al_2O_3-Hg junction at 1.07°K. The curve was obtained as a series of 120 discrete points. The scatter of the points is within the thickness of the line, so that it is appropriate to show the data in the form of a continuous curve. The I–V characteristic exhibits the expected negative resistance region preceded by a local maximum at $eV_-=(0.694\pm0.005)\times10^{-3}$ eV. The maximum does not have the form of a logarithmic singularity calculated from a BCS density of states given by

$$\begin{aligned}&\rho(E)=|E|/(E^2-\Delta^2)^{1/2}, \quad |E|\geq\Delta\\ &\rho(E)=0, \qquad\qquad\qquad |E|<\Delta.\end{aligned} \tag{1}$$

The current jump at the upper end of the negative resistance region is quite sharp, although the discontinuity which BCS predicts is absent. Therefore, a certain amount of ambiguity is introduced into selecting the voltage corresponding to $\Delta_{Hg}+\Delta_{Al}$. Somewhat arbitrarily, we have assumed that the point at which the slope of the I–V characteristic passes through a maximum indicates this voltage, so that $eV_+=\Delta_{Hg}+\Delta_{Al}=(0.95\pm0.03)\times10^{-3}$ eV. The indicated uncertainty represents the arbitrariness in the criterion for selecting V_+; other contributions to the uncertainty are negligible. At a given temperature, the positions of V_- and V_+ are repeatable to within ±0.005 mV from sample to sample. (Three samples were examined.) Solving for Δ_{Hg} and Δ_{Al}, we obtain for $T=1.07°K$,

$$\begin{aligned}\Delta_{Hg}&=(0.822\pm0.02)\times10^{-3}\text{ eV},\\ \Delta_{Al}&=(0.128\pm0.02)\times10^{-3}\text{ eV}.\end{aligned} \tag{2}$$

Using the BCS relation for $\Delta(T)/\Delta(0)$ versus T/T_c, we calculate fo rmercury $\Delta(1.07°)/\Delta(0)=0.9989$, where we have used the bulk critical temperature, $T_c=4.153°K$.

The width of the gap extrapolated to 0°K is therefore

$$\Delta_{Hg}(0)=(0.823\pm0.02)\times10^{-3}\text{ eV}, \tag{3}$$

which we multiply by two and express in terms of kT_c:

$$2\Delta_{Hg}(0)=(4.60\pm0.11)kT_c. \tag{4}$$

The actual T_c of the films were (4.15 ± 0.02)°K, which agrees with the bulk value used to obtain (4), within the limit of error.

This gap width for mercury, like the value of the other strong coupling superconductor, lead ($2\Delta_{Pb}(0)\simeq4.3\,kT_c$),[18–22] is appreciably greater than the value derived

[17] A. H. Wilson, *The Theory of Metals* (Cambridge University Press, London, 1954).

[18] I. Giaever and K. Megerle, Phys. Rev. **122**, 1101 (1961).

[19] S. Shapiro, P. H. Smith, J. Nicol, J. L. Miles, and P. F. Strong, IBM J. Res. Develop. **6**, 34 (1962).

[20] P. Townsend and J. Sutton, Phys. Rev. **128**, 591 (1962).

[21] J. D. Leslie and D. M. Ginsberg, Phys. Rev. **133**, A362 (1964).

[22] D. N. Douglass and R. Meservey (to be published).

on the basis of the BCS model in the weak-coupling approximation, $2\Delta(0)/kT_c=3.52$.[16] Our determination is in good agreement with the value $(4.6\pm0.2)kT_c$ obtained by Richards and Tinkham[23] in their measurements of the absorption of far infrared radiation in bulk mercury. In an indirect determination, Finnemore and Mapother[24] have obtained values for the mercury gap from measurements of the critical field curve. Using the BCS relation, $\Delta(0)=H_0(\pi k^2 v/6\gamma)^{1/2}$, where H_0 is the critical field at $T=0°$K, v the molar volume, and γ the electronic specific-heat coefficient, they calculate $2\Delta_{Hg}(0)/kT_c=3.96$. Fitting the shape of the electronic entropy curve, $S_{es}/\gamma T_c$ versus T/T_c, over a wide range of temperature, however, they deduce a value of 4.8. The discrepancy can be traced to the fact that the former calculation emphasizes the critical-field behavior at low reduced temperature, while the latter emphasizes the high-temperature behavior.

Rowell and Chynoweth[25] have performed tunneling studies on mercury frozen onto the surface of degenerate silicon, using the surface-barrier layer so formed as the insulating layer. They have published only an abstract, but claim that their results indicate a value for mercury of $2\Delta=(1.47\pm0.03)\times10^{-3}$ eV, which implies $2\Delta=4.1\ kT_c$. These results are necessarily those for the metal-insulator-superconductor junction, which do not provide as unambiguous a measure of the gap width as do our measurements on the superconductor-insulator-superconductor sandwich.

The discrepancy between our experimental value of the gap and the BCS value is of considerable interest. It can be shown that a solution of the BCS integral equation using a constant interaction, $V_{kk'}=V$ (BCS model), cannot give a value of $2\Delta(0)/kT_c$ greater than 4.00, the value for the strong-coupling limit $N(0)V=\infty$,[26] where $N(0)$ is the density of states at the Fermi surface in the normal state. A treatment that more adequately takes into account the strong electron-phonon interaction is probably needed. Schrieffer and Wada[27] have approached the problem using Green's function techniques. They find that as the temperature is increased, lifetime (damping) effects decrease the gap width below that predicted by BCS to an increasing extent, so that the transition temperature, where the gap vanishes, is reduced, thereby increasing the ratio $2\Delta(0)/kT_c$. The effect is particulary important in lead and mercury, where the electron-phonon coupling strength is unusually large.

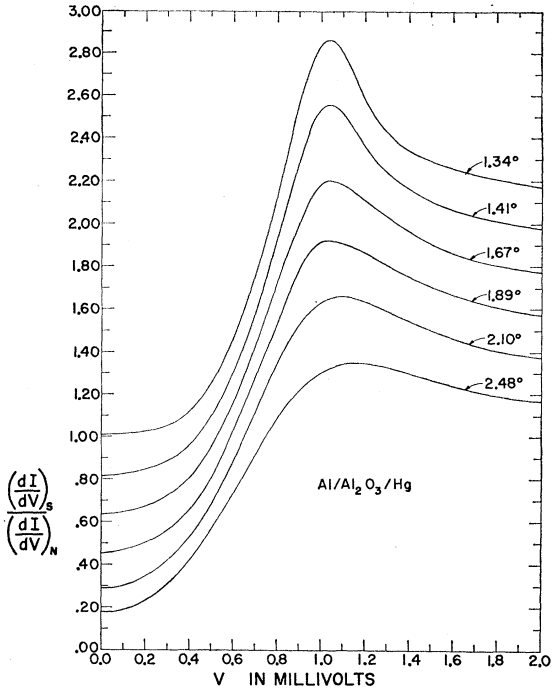

FIG. 3. The relative differential conductance versus bias voltage for six different temperatures. The aluminum film is in the normal state. The curves are successively displaced from one another by 0.2 vertical unit to clarify the behavior of the curves in the regions where they come close together. That is, the curve for 2.10°K is displaced upward by 0.2 unit, that for 1.89°K is displaced upward by 0.4 unit, etc.

Any attempt to estimate the amount or kind of smearing of the mercury gap edge indicated by the nondiscontinuous behavior of the I–V characteristic at $eV_+=\Delta_{Hg}+\Delta_{Al}$ is complicated by the fact that we do not know by how much the Al gap is smeared. If we assume that the smearing of the I–V curve at V_+ is due completely to the mercury, i.e., that the aluminum gap edge is perfectly sharp, we obtain a maximum value for the broadening of about (0.95−0.89) mV, or $\delta=0.06$ mV. A more realistic estimate, based on the available data for Al-Al_2O_3-Al sandwiches,[28] and on the character of the I–V curve in the vicinity of V_+, is $\delta\cong0.04$ mV, so that $\delta/\Delta_{Hg}\cong5\%$. Such smearing could come from several causes, among them: (1) nonuniform strains set up in the film, caused by the unequal rates of contraction of the metal and the quartz substrate upon cooling to liquid-helium temperature; (2) lifetime effects; (3) anisotropy of the gap. It should be noted that we do not expect to see serious effects due to the anisotropy, since the film thickness (about 1500 Å) is probably less than the bulk coherence length.[29]

[23] P. L. Richards and M. Tinkham, Phys. Rev. **119**, 575 (1960).
[24] D. K. Finnemore and D. E. Mapother (to be published); D. K. Finnemore, Ph.D. thesis, University of Illinois, 1962 (unpublished).
[25] J. M. Rowell and A. G. Chynoweth, Bull. Am. Phys. Soc. **7**, 473 (1962).
[26] J. C. Swihart, Phys. Rev. **131**, 73 (1963); IBM J. Res. Develop. **6**, 14 (1962).
[27] J. R. Schrieffer and Y. Wada, Bull. Am. Phys. Soc. **8**, 307 (1963); Y. Wada., Rev. Mod. Phys. **36**, 253 (1964).
[28] I. Giaever, H. R. Hart, Jr., and K. Mergerle, Phys. Rev. **126**, 941 (1962).
[29] P. W. Anderson, Phys. Chem. Solids **11**, 26 (1959).

IV. THE DENSITY OF STATES

A. The Region Near the Gap

The quantity most closely related to the superconducting density of states is the slope of the I–V characteristic with the tunneling sandwich in the metal-insulator-superconductor configuration. Giaever and Megerle, using a very simple model,[18] have obtained an expression for the tunneling current in terms of the density of states. They find for the general case of two metals, a and b, that

$$I=C_N/e\int_{-\infty}^{+\infty}\rho_a(E-eV)\rho_b(E)[f(E-eV)-f(E)]dE, \quad (5)$$

where C_N is the conductance with both metals in the normal state, ρ_a and ρ_b are the ratios of the density of states to that in the normal state, f is the Fermi function, e is the electronic charge, and V is the applied voltage. Specializing to the case where a is normal, $\rho_a=1$, and metal b is superconducting we obtain

$$\left(\frac{dI}{dV}\right)_S=C_N\int_{-\infty}^{+\infty}\rho_b(E)K(E,V)dE, \quad (6)$$

where the kernel, $K(E,V)$, is given by

$$K(E,V)=\frac{1}{kT}\frac{\exp[(E-eV)/kT]}{\{\exp[(E-eV)/kT]+1\}^2}. \quad (7)$$

$K(E,V)$ is a bell-shaped curve, symmetrically peaked about the value $E=eV$, whose full width at half-maximum is approximately $3.5\,kT$. At $T=0$°K, $K(E,V)$ becomes a delta function, and dI/dV should be directly proportional to the superconducting density of states. For $\rho_b(E)$ equal to a BCS density of states (1), tables have been computed with the help of a digital computer which give $(dI/dV)_S/C_N$ as a function of eV/Δ and Δ/kT.[30]

We have measured the slope of the characteristic directly by sending a small 1000-cps ac current from a high impedance source through the film junction and recording the ac voltage across the junction, which is proportional to dV/dI. Figure 3 shows a plot of $(dI/dV)_S$, the differential conductance with the mercury film in the superconducting state, divided by $(dI/dV)_N$, the differential conductance with the mercury film in the normal state, versus the bias voltage V. Curves are shown for six different temperatures between 1.34 and 2.48°K, and are successively displaced by 0.2 vertical unit to avoid confusion in the regions where the curves come together. The maximum applied ac voltage is 10 μV peak-to-peak. Curves were obtained for two samples, and were repeatable at a given temperature to within ± 0.005 mV on the horizontal axis, and to $\pm 1\frac{1}{2}\%$ on the vertical axis. Very small leakage currents were observed, the leakage conductance being 1/600th of the normal-state conductance. These leakage currents were subtracted out in plotting the graphs.

Figure 4 shows a comparison of the experimental first derivative curve at the lowest temperature at which the first derivative was measured ($T=1.34$°K), with the theoretical tunneling curve obtained from the BCS density of states (1) with $\Delta=0.818$ mV. This value of Δ is obtained from the superconductor-insulator-superconductor characteristic, and has been adjusted for temperature by using the BCS relation for $\Delta(T)$ versus T; i.e., $\Delta(1.34)=0.995\ \Delta(0)=(0.995)(0.823)=0.818$ mV. The qualitative agreement between the experimental and theoretical tunneling curves is good, although the discrepancies are far outside the experimental error. The experimental curve is seen to be more strongly peaked and to have a larger tail at low bias voltage. The use of different values of Δ does not improve the over-all agreement. For example, a Δ of 0.86 mV gives a fairly good fit in the region of steep slope around 0.8 mV, but produces values too low by 30–40% for voltages below about 0.6 mV. On the other hand, a Δ of 0.79 mV, which gives good agreement in the low-voltage region, yields a much poorer fit in the region of the gap (e.g., 25% too high at 0.8 mV) and at higher voltages. Even with $\Delta=0.86$ mV, the height of the peak in the experimental curve exceeds that of the BCS curve by 0.15 unit, or about 9%.

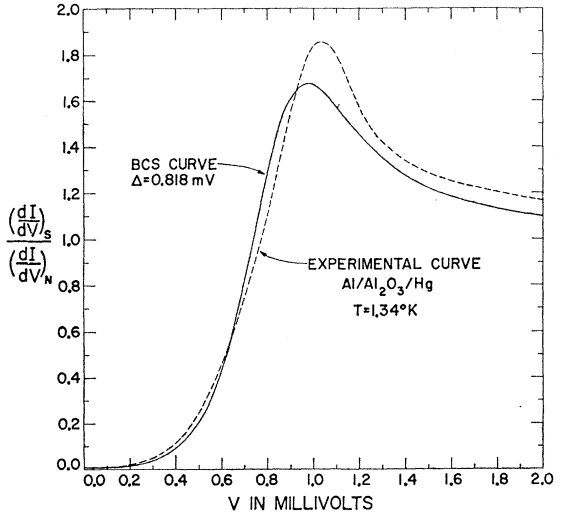

FIG. 4. Comparison of the experimental and theoretical relative differential conductance curves plotted against bias voltage for $T=1.34$°K. The theoretical curve was calculated using the BCS density-of-states function with a value for Δ which was obtained from the superconductor-insulator-superconductor I–V characteristic, corrected for temperature using the BCS gap-versus-temperature relation. The aluminum is in the normal state.

[30] S. Bermon, Technical Report No. 1 on National Science Foundation Grant NSF GP1100, Physics Department, University of Illinois, 1964 (unpublished). This report contains tabulated values of $(dI/dV)_S/(dI/dV)_N$ calculated from the BCS theory for $0.4\leq\Delta/kT\leq 49.5$ and $0\leq(eV/\Delta)\leq 20$, to four significant figures.

Notice that for higher voltages, the experimental first derivative curve continues to exceed the BCS curve. They finally cross at 3.3 mV, beyond the range of the graph. Thus, it appears that the experimental density of states is appreciably higher than the BCS density of states in that region starting somewhat above the gap to at least three times the gap.

The behavior in the vicinity of the gap is more difficult to understand. An effort was made to calculate a density of states function by solving Eq. (6) for $\rho(E)$ with $(dI/dV)_S/(dI/dV)_N$ given by the data from $T=1.34$°K. Unfortunately, even at this temperature the full width at half-maximum of $K(E,V)$ is still approximately one-half of the gap width. As a result, it is impossible to resolve the form of the density of states in the rapidly changing region near the gap edge; a variety of peak shapes provide agreement with the tunneling curve within the experimental error. For this reason, solutions so obtained are not considered to be useful. A common feature of such solutions, though, is that those which give reasonable agreement with the dI/dV data, for voltages in the vicinity of the gap and above, underestimate dI/dV by a large percentage for lower voltages unless a substantial number of states are included below the gap. There is, however, no indication from the behavior of the superconductor-insulator-superconductor tunneling characteristic that there exist states below the gap. It is possible that processes other than those described by Eq. (6) are taking place, and increase the differential conductance, such effects being particularly important in the low voltage range, where the differential conductance is already small. Taylor and Burstein,[13] for example, have discovered both temperature-dependent and temperature-independent excess currents (other than those attributed to double particle processes) in their lead tunneling samples. An explanation of the temperature-dependent part as due to phonon-assisted tunneling has been put forth by Kleinman.[12] It would appear, however, that if mercury is at all like lead in these respects, such currents are too small to account for the discrepancies here.

B. The Density of States at Higher Energies; The Phonon Spectrum

The behavior of the differential conductance at higher bias voltages is also of considerable interest. Schrieffer, Scalapino, and Wilkins[10] have examined the problem of tunneling into superconductors using Green's function techniques. They are able to include the dynamic interactions between phonons and electrons in a consistent manner, and arrive at results that are particularly important for the strong-coupling superconductors, such as lead and mercury, in which the electron-phonon interaction is sufficiently strong that the quasiparticle approximation breaks down. They obtain an equation for the tunneling current that is similar to Eq. (6) except that $\rho(E)$, the usual quasiparticle density of states, is replaced by an *effective tunneling density of states* $N_T(E)$, which is directly related to the one-particle Green's function, and which is given explicitly by

$$\frac{N_T(E)}{N(0)}=\mathrm{Re}\left\{\frac{|E|}{[E^2-\Delta^2(E)]^{1/2}}\right\}, \tag{8}$$

where $\Delta(E)=\Delta_1(E)+i\Delta_2(E)$ is the complex energy-gap parameter. Moreover, they find that at each energy corresponding to a peak in the phonon spectrum there is a rapid increase in the imaginary part of the energy-gap parameter associated with a shortened lifetime. This produces a sharp drop in $N_T(E)$, and consequently in the differential conductance $(dI/dV)_S$. Thus, we expect to observe structure in the tunneling curves related to structure in the phonon spectrum. Such structure has indeed been observed in lead by Giaever, Hart, and Megerle,[28] and in lead and tin by Rowell, Anderson, and Thomas.[31] Rowell, with the aid of neutron scattering data for lead, has been able to associate the structure in the conductance characteristic with transverse and longitudinal peaks in the phonon density of states.

We have measured the differential conductance in the region of higher bias voltage with the intent of observing such structure for mercury. Figure 5 shows a plot of $(dI/dV)_S/(dI/dV)_N$ versus bias voltage for V between

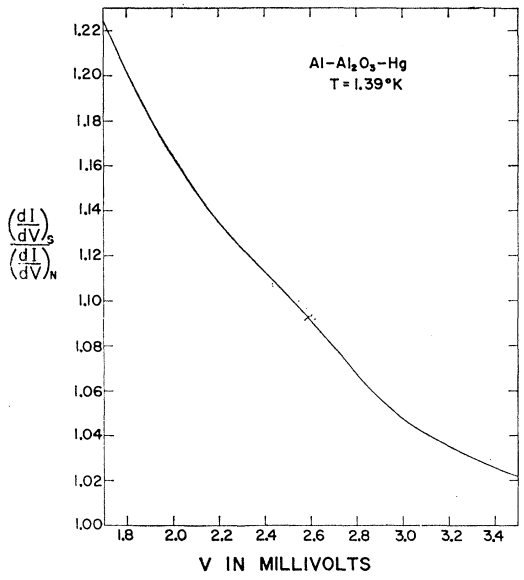

FIG. 5. The relative differential conductance versus bias voltage at $T=1.39$°K for V in the range from 1.7 to 3.5 mV. The aluminum is in the normal state. The experimental curve crosses at 3.3 mV the theoretical curve (not shown) calculated using the BCS density of states function with a value for Δ obtained from the superconductor-insulator-superconductor I–V characteristic, corrected for temperature using the BCS gap-versus-temperature relation. The theoretical curve is smaller than the experimental curve for $V<3.3$ mV.

[31] J. M. Rowell, P. W. Anderson, and D. E. Thomas, Phys. Rev. Letters **10**, 334 (1963).

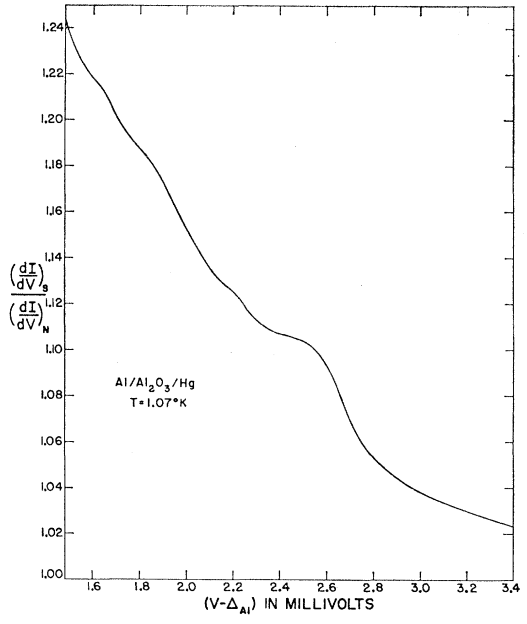

FIG. 6. The relative differential conductance versus $(V-\Delta_{Al})$ at $T=1.07°K$ for $(V-\Delta_{Al})$ in the range from 1.58 to 3.4 mV. The aluminum is in the superconducting state with $\Delta_{Al}=0.13$ mV.

1.7 and 3.5 mV. The maximum ac voltage across the junction is 60 μV peak-to-peak. The aluminum is in the normal state. The broad hump in the curve around 2.6 mV, although not pronounced, is unmistakable. It is important to point out, however, that the thermal smearing at this temperature is still considerable [the half-width of $K(E,V)=0.42$ mV], so that structure of comparable or smaller width would be obscured.

A more effective method for resolving the structure is to measure dI/dV with the aluminum as well as the mercury in the superconducting state, thus making use of the sharp peak at the edge of the gap in the aluminum superconducting density of states to probe the structure in the mercury density of states. The results of such a measurement at $T=1.07°K$ are shown in Fig. 6, where $(dI/dV)_S/(dI/dV)_N$ is plotted against $(V-\Delta_{Al})$ The maximum ac applied voltage is still 60 μV peak-to-peak. The structure in the curve in the vicinity of 2.6 mV which in Fig. 5 is only a gentle variation, is quite pronounced in this plot. Moreover, irregularities in the curve at about 1.6, 1.8, and 2.1 mV are now evident.

The behavior of $(dI/dV)_S/(dI/dV)_N$ versus $(V-\Delta_{Al})$ for V between 4.0 and 23 mV is shown in Fig. 7. The applied ac voltage is 190 μV peak-to-peak. The variations in the curve in this range are seen to be quite small (less than 1%) and relatively broad. In fact, the structure is so broad in this region that the effect of thermal smearing is unimportant, and the same curve is obtained whether the aluminum is in the superconducting or in the normal state. Thus, Fig. 7 should represent rather accurately the effective tunneling density of states in this energy region for mercury.

The dependence shown in Fig. 7 was repeated in many runs on three different samples, to within $\pm 2\%$ of full scale in the vertical direction and to ± 0.1 mV in the horizontal direction. For Fig. 6, measurements were made on only one sample, so that sample-to-sample comparisons cannot be made, although the curve was repeatable from run to run to within $\pm 1\%$ full scale. The irregularity in Fig. 5 was observed in all three samples.

Before continuing, it is important to mention the behavior of the differential conductance with the mercury film in the normal state, $(dI/dV)_N$. According to the present theory,[7] the tunneling current should be a linear function of the voltage, $I=C_N V$, for small voltages, and thus $(dI/dV)_N$ should be a constant, independent of the bias voltage. Experimentally this was not found to be the case. Figure 8 presents a plot of $(dV/dI)_N$, the inverse of $(dI/dV)_N$, as a function of voltage from 0 to 40 mV. (The graph is traced directly from the chart recorder, whose output is proportional to the ac resistance.) The curve was obtained at 4.2°K, slightly above the critical temperature of the mercury film. The same curve was obtained for $T=1.4°K$ when the mercury was forced into the normal state by the application of a magnetic field of 3000 Oe.

It is seen that $(dV/dI)_N$ is not constant, but decreases by about $2\frac{1}{2}\%$ in 40 mV. Moreover, the curve is not symmetrical about the origin. In Fig. 8, the mercury film is biased positive. If the positive bias is applied to aluminum film, a similar curve is obtained, but multiplied by a factor of about 1.7. This normal state behavior is closely repeatable ($\pm 2\%$ of full scale) from run to run, and from sample to sample. It is not due to heating caused by increased current passing through film, since the entire change in the junction resistance as the film is warmed from 4 to 77°K is less than $2\frac{1}{2}\%$.

Fisher and Giaever[32] have found an Ohmic behavior

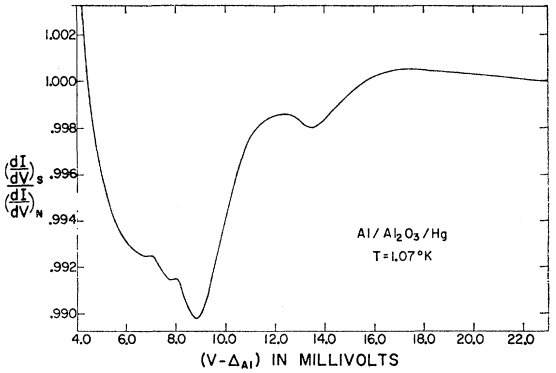

FIG. 7. The relative differential conductance versus $(V-\Delta_{Al})$ at $T=1.07°K$ for $(V-\Delta_{Al})$ in the range from 4.0 to 23.0 mV. The aluminum is in the superconducting state with $\Delta_{Al}=0.13$ mV. This same curve is obtained at $T=1.39°K$, where the aluminum is in the normal state ($\Delta_{Al}=0$).

[32] J. C. Fisher and I. Giaever, J. Appl. Phys. **32**, 172 (1961).

for normal Al-Al_2O_3-Al sandwiches at low voltages (below about 50 mV), and an exponential rise in current at higher voltages (above about 200 mV). It should be pointed out that the deviation from linearity observed here would barely be discernible on a graph with a size equal to that of the one presented in their paper.

Notice that for bias voltages greater than 4 mV the variations in the superconducting and in the normal state differential conductances are comparable. A plot of $(dI/dV)_S$ uncorrected for the normal state variation is substantially different from the graph presented in Fig. 7. Moreover, since $(dI/dV)_N$ is asymmetrical about the origin, one would expect that $(dI/dV)_S$ be asymmetrical. This is indeed so. However, when the ratio $(dI/dV)_S/(dI/dV)_N$ is taken, the resulting curve is the same for both polarities. This satisfying result implies that it is indeed the relative conductance, $(dI/dV)_S/(dI/dV)_N$, that is the important quantity in determining the reduced density of states of the superconductor, despite the fact that $(dI/dV)_N$ is not a constant. Further support is given by the fact that the normal and superconducting dI/dV curves coincide for bias voltages greater than about 23 mV. That is, the reduced density of states calculated from $(dI/dV)_S/(dI/dV)_N$ does indeed go to unity for sufficiently high energy.

A particularly useful and sensitive method for investigating the structure in the effective tunneling density of states is to determine the behavior of the second derivative of the tunneling current, d^2I/dV^2. The sharp drops in dI/dV, which are thought to correspond to peaks in the phonon distribution, appear as relative minima, or negative peaks, in d^2I/dV^2, whose position are easy to determine. Moreover, structure barely discernible in the first derivative may show up quite clearly in the second.

We have measured the second derivative by observing the second harmonic component of voltage generated by a sinusoidal current passing through the film junction. Because we use a constant current source, the second harmonic output is proportional to d^2V/dI^2. One commonly plots d^2I/dV^2. This is calculated from the identity, $d^2I/dV^2=-(d^2V/dI^2)/(dV/dI)^3$.

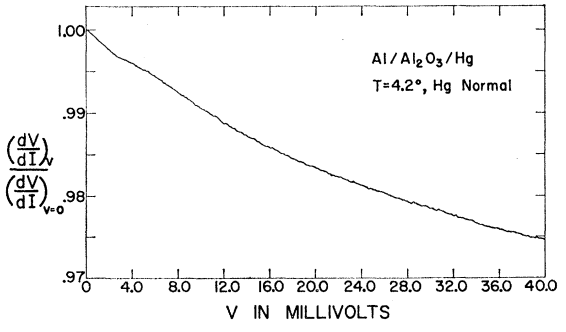

FIG. 8. The differential *resistance* of an Al-Al_2O_3-Hg junction with both the mercury film and the aluminum film in the normal state, normalized to the value at $V=0$.

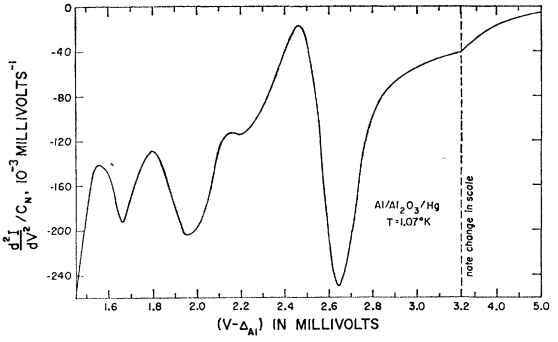

FIG. 9. Plot of $(d^2I/dV^2)/C_N$ versus $(V-\Delta_{Al})$ at $T=1.07$°K for $(V-\Delta_{Al})$ in the range from 1.45 to 5.00 mV. d^2I/dV^2 is divided by C_N, the average value of the normal state conductance, in order to normalize it. The aluminum is superconducting with $\Delta_{Al}=0.13$ mV. To relate the structure in the curve to possible structure in the phonon spectrum, subtract the mercury gap, $\Delta_{Hg}(1.07°)=0.822$ mV. (See text.)

Figure 9 shows a plot of $(d^2I/dV^2)/C_N$ versus $(V-\Delta_{Al})$ for $(V-\Delta_{Al})$ in the range between 1.45 and 5.00 mV. Both metals are superconducting. The maximum voltage across the junction is 145 μV peak-to-peak. d^2I/dV^2 is divided by C_N, the average value of the normal state conductance, in order to normalize it.

A plot of the second derivative for the region between 5.0 and 20.0 mV is shown in Fig. 10. The applied ac voltage is 630 μV peak-to-peak. The graph was taken directly from the chart recorder, and so is actually proportional to $-d^2V/dI^2$. The maximum error involved, however, in approximating d^2I/dV^2 by a quantity proportional to d^2V/dI^2 in this range, where the variation of dV/dI is so small, is only $1\frac{1}{2}\%$, and is considered a small price to pay in order to preserve all the structure in the curve.

Figure 9 is reproducible from run to run to within $\pm 3\%$ of full scale on the vertical axis and to ± 0.03 mV on the horizontal axis. The corresponding numbers for Fig. 10 are $\pm 3\%$, and ± 0.1 mV. Second derivative curves were obtained for one sample only.

Notice that the size of the second derivative peaks in the energy range of Fig. 10 are nearly two orders of magnitude smaller than the size of the peaks in the range defined by Fig. 9, and also that the structure in the higher energy region is considerably broader than that in the higher energy region is considerably broader than that in the low energy region.

As already mentioned, structure similar to that seen in this experiment has been observed in lead by Rowell *et al.*,[31] who have interpreted it in conjunction with neutron scattering data for lead. They identify a set of peaks in the second derivative around 4.5 mV and a set at 8.5 mV with transverse and longitudinal phonons, respectively. It is also claimed that harmonic and sum frequencies of these two groups can be seen at higher biases. Furthermore, Scalapino and Anderson[33] have

[33] D. J. Scalapino and P. W. Anderson, Phys. Rev. **133**, A921 (1964).

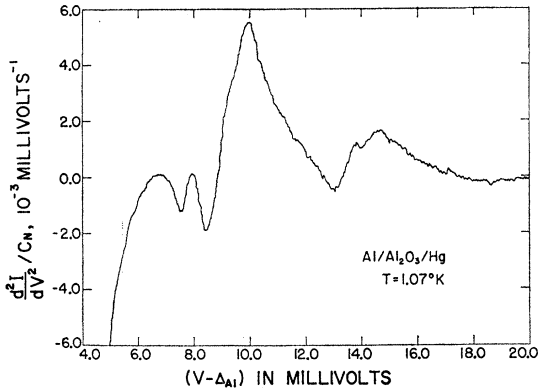

FIG. 10. $(d^2I/dV^2)/C_N$ versus $(V-\Delta_{Al})$ at $T=1.07°K$ for $(V-\Delta_{Al})$ in the range from 5.0 to 20.0 mV. The aluminum is superconducting with $\Delta_{Al}=0.13$ mV. To relate the structure in the curve to possible structure in the phonon spectrum, subtract the mercury gap, $\Delta_{Hg}(1.07°)=0.822$ mV. (See text.)

shown that d^2I/dV^2 in the superconductor-insulator-superconductor junction should exhibit inverse square-root or logarithmic singularities at energies corresponding to Van Hove singularities[34,35] in the phonon spectrum. Rowell's curves, like the present ones for mercury, exhibit no such singularities, possibly because of the smearing of the gap edge.[35a] Rowell is, however, able to identify points of steep slope in dI^2/dV^2 with the positions of the Van Hove singularities obtained from the lead neutron data.

Unfortunately, no neutron scattering experiments have been performed on mercury, nor have any theoretical attempts apparently been made to calculate the phonon spectrum. Thus we have nothing with which to compare our data. How plausible is it that the observed structure is due to phonons? According to the theory,[10] phonon peaks at energies ω_q produce the sharp drops in the effective tunneling density of states at energies $\omega_q+\Delta_0$, where Δ_0 is the gap parameter at the edge of the energy gap. Thus for the purpose of determining possible positions of phonon peaks we present in Table I the values of $(V-\Delta_{Al}-\Delta_{Hg})$, expressed in millivolts and in degrees Kelvin, for the negative peaks in d^2I/dV^2 obtained from Figs. 9 and 10.

TABLE I. Energies at which minima occur in the tunneling current's second derivative with respect to voltage.

Peak No.	$V-\Delta_{Al}-\Delta_{Hg}$ mV	°K
1	0.84	9.7
2	1.14	13.2
3	1.38	16.0
4	1.82	21.1
5	6.7	78
6	7.6	88
7	12.2	142

Measurements of the specific heat[36,37] indicate that the Debye temperature θ_D for mercury shows a very strong variation with temperature below $T=80°K$. Even down to 1.2°K, no T^3 region in the specific heat is observed. Gruneisen and Hoyer[38] have used the elastic constants measured at 80°K to calculate θ_D. They obtain a value of 68°K, which would refer to the value of genuine T^3 region, provided the elastic constants do not change appreciably from 80 to 0°K. This value is in reasonable agreement with the above calorimetric data.

If we do assume $\theta_D=68°K$, we note that the energies of peaks No. 1 (9.7°) and 2 (13.2°) are 0.14 and 0.19, respectively, of the Debye energy. We might not ordinarily expect to see peaks in the phonon spectrum at quite such a low energy, although mercury may be unusual in this respect. On the other hand, that the large peak (No. 4) at 21.1°K is due to a phonon peak is quite reasonable. Simon[39] has shown, in fact, that his specific heat data could be well represented by the sum of a Debye function with $\theta_D=120°K$, and an Einstein function with $\theta_E=25°K$, a value not too different from the above. Nevertheless, the fact remains that detailed information on the phonon spectrum of mercury, whether obtained from neutron scattering data or otherwise, is needed to make certain the origin of the observed structure in these tunneling curves.

The d^2I/dV^2 curves have also been examined for the presence of harmonic and sum frequencies. Note that no structure was observed in the region from about $(V-\Delta_{Al}-\Delta_{Hg})=2.2$ to 4.5 mV, where simple sums and low-order harmonics of the first four possible phonon frequencies would be expected to occur. We conclude, therefore, that the structure at higher energies, if it can be attributed to phonon processes at all, probably does not represent sums or harmonics of low-frequency phonons, but corresponds to actual peaks in the phonon spectrum.

V. TEMPERATURE DEPENDENCE OF THE GAP WIDTH

The relative differential conductance at zero bias voltage, $\sigma_0\equiv(dI/dV)_S/(dI/dV)_N$ at $V=0$, in the metal-insulator-superconductor configuration, has been used to estimate the temperature dependence of the energy gap. It is at $V=0$ that $(dI/dV)_S$ varies most rapidly as the gap is varied; thus σ_0 is particularly appropriate for determining that variation, and moreover is simply measured. If we assume a BCS density of states (1),

[34] L. Van Hove, Phys. Rev. **89**, 1189 (1953).
[35] J. C. Phillips, Phys. Rev. **104**, 1263 (1956).
[35a] *Note added in proof*. The high-voltage wing of the structure at about 2.6 mV in Fig. 9 can be well fitted by an inverse square root singularity centered at 2.71 mV. It cannot be fitted by a logarithmic singularity.
[36] P. L. Smith and N. M. Wolcott, Phil. Mag. **1**, 854 (1956).
[37] R. H. Busey and W. F. Giauque, J. Am. Chem. Soc. **75**, 806 (1953).
[38] E. Gruneisen and H. Hoyer, Ann. Physik **22**, 663 (1935).
[39] F. E. Simon, Z. Physik. Chem. **107**, 279 (1923); Ann. Physik **68**, 241 (1922).

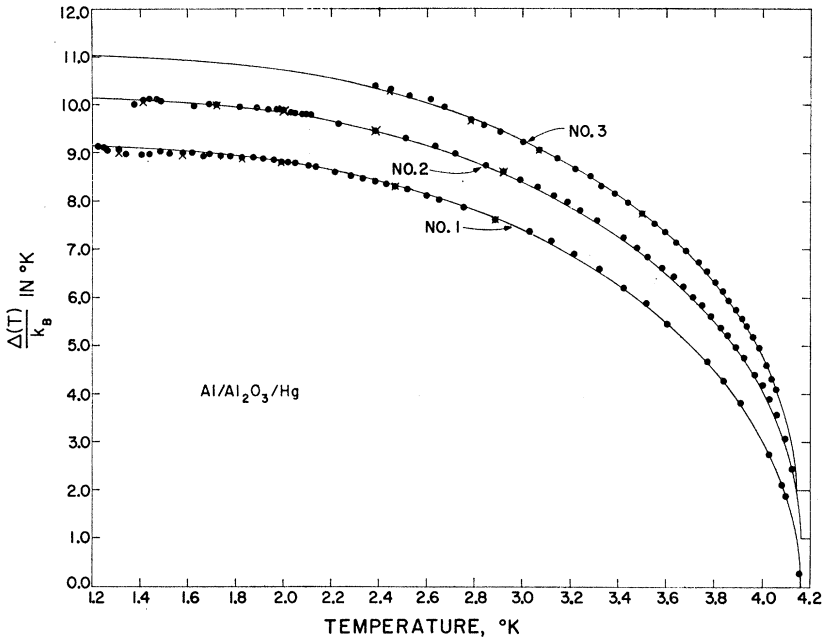

FIG. 11. The solid dots show the temperature variation of the mercury superconducting energy gap for three different samples, as indicated by the ac conductance at zero bias voltage. For clarity, curve No. 2 is displaced upward by one unit, and curve No. 3 is displaced upward by two units. The solid lines represent the BCS temperature variation of the gap, but with $\Delta(0)$ adjusted to give the best visual fit of the theoretical curve to the data; i.e., the BCS curve has been scaled by the constant factor, $\Delta(0)/1.76\ k_BT_c$. The values of $\Delta(0)$ are: Nos. 1 and 2, $\Delta(0)/k_B=9.15$°K; No. 3, $\Delta(0)/k_B=9.04$°K. These values should not be taken as absolute measures of the gap, for the reasons explained in the text. The critical temperatures of the samples are: Nos. 1 and 2, $T_c=4.16$°K; No. 3, $T_c=4.14$°K. The leakage conductance, calculated from the zero-bias conductance at the lowest temperature, has been compensated for in calculating the position of the experimental points. To indicate the extent of such corrections, some of the uncorrected points are shown (indicated by crosses) along with the corrected points. Except for the very low reduced temperatures, the corrections are seen to be negligible.

allowing Δ to be an unknown parameter, then σ_0 becomes solely a function of the gap divided by the temperature, $\alpha=\Delta/kT$, and may be expressed in the form[30]

$$\sigma_0'(\alpha)=2\int_0^\infty \exp(x^2+\alpha^2)^{1/2}/[\exp(x^2+\alpha^2)^{1/2}+1]^2dx, \quad (9)$$

where the prime denotes the fact that we have used a BCS density of states.

Employing (9) to calculate Δ from the measured values of σ_0' assumes that the density of states is of the BCS form—which we saw is only approximately consistent with measurements of dI/dV over the whole voltage range. The absolute values of the gap obtained in this way will not be correct, the extrapolated zero temperature gap being from 4 to 6% lower than the value obtained from the I–V characteristic with both metals superconducting. Nevertheless, the procedure is still useful. For even if it does not predict the gap itself accurately, it may give us an idea of the manner in which the gap varies with temperature.

Figure 11 shows the results obtained from three different samples. The gap is plotted along the vertical scale in units of temperature. The curves are displaced from one another by one vertical unit to avoid confusion.

The solid lines are the theoretical weak-coupling BCS curves for the variation of the gap with temperature, scaled by the constant multiplier $2\Delta(0)/(3.52\ kT_c)$. $\Delta(0)$ for each sample is picked to give the best visual fit to the experimental points. The agreement of the "experimental" points with the scaled BCS curves is seen to be quite good, although this may in part be a consequence of our freedom in selecting a value of $\Delta(0)$.

VI. SUMMARY OF CONCLUSIONS

The width of the energy gap at $T=0$°K in superconducting films of mercury has been determined to be $2\Delta(0)=(1.65\pm0.04)\times10^{-3}$ eV$=(4.60\pm0.11)k_BT_c$ from measurements of the current voltage characteristic with the tunneling junction in the superconductor-insulator-superconductor configuration. This value is in excellent agreement with the gap width found by Richards and Tinkham from their measurements of the absorption of far infrared radiation in bulk mercury $[2\Delta(0)/k_BT_c=4.6\pm0.2]$. It exceeds the value predicted by the BCS theory in the weak-coupling limit $[2\Delta(0)/k_BT_c=3.52]$ by a significant amount, probably because of the strong electron-phonon interaction which which exists in mercury. The smearing of the gap edge as indicated by the nondiscontinuous jump in the current at the upper end of the negative-resistance region is estimated to be 0.04×10^{-3} eV, or about 5% of the gap width.

Measurements of the differential conductance in the vicinity of the gap in the metal-insulator-superconductor junction show qualitative agreement with tunneling curves calculated from a BCS density of states, but the experimental curves are more peaked and have a larger tail at low bias voltages. The data indicate that in the range from slightly above the gap to at least three times the gap the actual density of states appreciably exceeds the BCS density of states. Due to thermal smearing, the behavior of the density of states in the vicinity of the gap could not be accurately determined; for this purpose much lower reduced temperatures are needed. A project is already in progress in this laboratory to extend our work down to 0.3°K.

The dependence of the gap width on temperature has been estimated from the differential conductance at zero bias voltage. Good agreement is found with the predicted BCS variation if the BCS curve is scaled by a constant multiplier to give the best visual fit to the data.

Structure, thought to indicate peaks in the phonon spectrum of mercury, has been observed in the first and second derivatives of the tunneling characteristic. d^2I/dV^2 exhibits two groups of minima, one group at low energies, in which the peaks are relatively large and sharp, and a second group at higher energies, in which the structure is small and broad. Neutron scattering experiments performed on mercury might provide further information about these peaks.

ACKNOWLEDGMENTS

We are grateful to J. Bardeen, L. P. Kadanoff, J. R. Schrieffer, and J. W. Wilkins for valuable discussions regarding the interpretation of the experimental results.

PHYSICAL REVIEW VOLUME 135, NUMBER 2A 20 JULY 1964

Double-Resonance Phenomena in the Gaseous Laser*

W. CULSHAW

Research Laboratories, Lockheed Missiles and Space Company, Palo Alto, California

(Received 20 February 1964)

The theory of double-resonance phenomena, or the simultaneous action of optical transitions and rf perturbations between the Zeeman sublevels of an atom, is extended to the induced emission and absorption processes effected by the monochromatic radiation and the discrete resonances involved in the gas laser. Expressions for the probability amplitudes of the Zeeman sublevels under such conditions are derived from time-dependent perturbation theory, the lifetimes of the states being introduced in a phenomenological way. Zeeman splittings of both upper and lower states involved in the laser transition are considered, and an effective term diagram used to discuss the results. Small signal approximations are applied to consider some specific cases, which show that the light beats seen in spontaneous emission when the rf frequency ω_0 equals the Larmor frequency, and in other instances, do not occur in induced emission unless such frequencies coincide with axial resonances of the laser cavity. Variations in the intensity and resonance effects are indicated at Zeeman splittings corresponding to ω_0, with similar variations in the amplitude of any beat frequencies due to multiple axial resonances. Additional coherence effects occur where levels cross, which will give rise to changes in the intensity and polarization of the induced emission at the corresponding frequency.

1. INTRODUCTION

THE use of double-resonance phenomena for the investigation of atomic structure was first discussed by Bitter[1] with reference to measurements on the hyperfine structure of excited atomic states. Some clarification of the original ideas was also given later by Pryce.[2] In double-resonance experiments, atoms are subjected simultaneously to radiations at both optical and radio frequencies, which are near to the atomic resonant frequencies involved in electric dipole and magnetic dipole transitions, respectively. Experiments on the effect of such rf perturbations between the Zeeman sublevels of an excited state were proposed by Brossel and Kastler,[3] and the first experiment on such double-resonance phenomena was done by Brossel and Bitter[4] using mercury vapor situated in a uniform magnetic field. Here suitable optical resonance radiation excited the mercury atoms from the ground state $^1S_0$ to the state $m=0$ of the excited state $^3P_1$, the wavelength being 2537 Å. Transitions to the states $m=\pm1$ were then induced by an rf magnetic field oscillating perpendicularly to the dc magnetic field at the Larmor frequency. These rf transitions were detected by the changes they produced on the intensity and polarization of the spontaneously emitted optical radiation. Resonance curves showing the variation of light intensity with dc magnetic field at a given rf frequency were obtained. From these curves quite accurate values of the g factor of the excited state were deduced, and the width of such resonances at low rf field amplitudes represented a measure of the natural linewidth of the excited state.

Dodd *et al.*[5] later did similar experiments which showed that the fluorescent light in such a double-resonance experiment is strongly modulated at the Larmor frequency and at multiples of this, depending on the dc magnetic field and on the orientations of the incident and observed polarizations of the optical radiation. Such modulation effects are due to beats between the spontaneously emitted radiations at

* Research on report supported by the Independent Research Program of Lockheed Missiles and Space Company.

[1] F. Bitter, Phys. Rev. **76**, 833 (1949).

[2] M. H. L. Pryce, Phys. Rev. **77**, 136 (1950).

[3] J. Brossel and A. Kastler, Compt. Rend. **229**, 1213 (1949).

[4] J. Brossel and F. Bitter, Phys. Rev. **86**, 308 (1952).

[5] J. N. Dodd, W. N. Fox, G. W. Series, and M. J. Taylor, Proc. Phys. Soc. (London) **74**, 789 (1959).